

## International Journal of Remote Sensing

Publication details, including instructions for authors and subscription information:

<http://www.tandfonline.com/loi/tres20>

### Evaluation of pre/post-fire differenced spectral indices for assessing burn severity in a Mediterranean environment with Landsat Thematic Mapper

Sander Veraverbeke<sup>a b</sup>, Stefaan Lhermitte<sup>c</sup>, Willem W. Verstraeten<sup>d</sup> & R. Goossens<sup>a</sup>

<sup>a</sup> Department of Geography, Ghent University, Ghent, Belgium

<sup>b</sup> Jet Propulsion Laboratory, California Institute of Technology, Pasadena, CA, USA

<sup>c</sup> Centro de Estudios Avanzados en Zonas Aridas (CEAZA), Universidad de la Serena, La Serena, Chile

<sup>d</sup> Geomatics Engineering, Katholieke Universiteit Leuven, Leuven, Belgium

Available online: 28 Jun 2011

To cite this article: Sander Veraverbeke, Stefaan Lhermitte, Willem W. Verstraeten & R. Goossens (2011): Evaluation of pre/post-fire differenced spectral indices for assessing burn severity in a Mediterranean environment with Landsat Thematic Mapper, International Journal of Remote Sensing, 32:12, 3521-3537

To link to this article: <http://dx.doi.org/10.1080/01431161003752430>

PLEASE SCROLL DOWN FOR ARTICLE

Full terms and conditions of use: <http://www.tandfonline.com/page/terms-and-conditions>

This article may be used for research, teaching and private study purposes. Any substantial or systematic reproduction, re-distribution, re-selling, loan, sub-licensing, systematic supply or distribution in any form to anyone is expressly forbidden.

The publisher does not give any warranty express or implied or make any representation that the contents will be complete or accurate or up to date. The accuracy of any instructions, formulae and drug doses should be independently verified with primary sources. The publisher shall not be liable for any loss, actions, claims, proceedings, demand or costs or damages whatsoever or howsoever caused arising directly or indirectly in connection with or arising out of the use of this material.

## Evaluation of pre/post-fire differenced spectral indices for assessing burn severity in a Mediterranean environment with Landsat Thematic Mapper

SANDER VERAVERBEKE<sup>\*†‡</sup>, STEFAAN LHERMITTE<sup>§</sup>,  
WILLEM W. VERSTRAETEN<sup>¶</sup> and R. GOOSSENS<sup>†</sup>

<sup>†</sup>Department of Geography, Ghent University, Ghent, Belgium

<sup>‡</sup>Jet Propulsion Laboratory, California Institute of Technology, Pasadena, CA, USA

<sup>§</sup>Centro de Estudios Avanzados en Zonas Aridas (CEAZA), Universidad de la Serena,  
La Serena, Chile

<sup>¶</sup>Geomatics Engineering, Katholieke Universiteit Leuven, Leuven, Belgium

(Received 4 February 2009; in final form 27 July 2009)

In this study several pre/post-fire differenced spectral indices for assessing burn severity in a Mediterranean environment are evaluated. GeoCBI (Geo Composite Burn Index) field data of burn severity were correlated with remotely sensed measures, based on the NBR (Normalized Burn Ratio), the NDMI (Normalized Difference Moisture Index) and the NDVI (Normalized Difference Vegetation Index). In addition, the strength of the correlation was evaluated for specific fuel types and the influence of the regression model type is pointed out. The NBR was the best remotely sensed index for assessing burn severity, followed by the NDMI and the NDVI. For this case study of the 2007 Peloponnese fires, results show that the GeoCBI-dNBR (differenced NBR) approach yields a moderate–high  $R^2 = 0.65$ . Absolute indices outperformed their relative equivalents, which accounted for pre-fire vegetation state. The GeoCBI-dNBR relationship was stronger for forested ecotypes than for shrub lands. The relationship between the field data and the dNBR and dNDMI (differenced NDMI) was nonlinear, while the GeoCBI-dNDVI (differenced NDVI) relationship appeared linear.

### 1. Introduction

Wildfires play a major role in Mediterranean type ecosystems (MTEs) (Pausas 2004) as they partially or completely remove the vegetation layer and affect post-fire vegetation composition, water and sediment regimes, and nutrient cycling (Kutiel and Inbar 1993). As such they act as a natural component in vegetation succession cycles (Trabaud 1981, Capitanio and Carcaillet 2008) but also potentially increase degradation processes, such as soil erosion (Thomas *et al.* 1999, Fox *et al.* 2008). Assessment of the fire impact is thus a major challenge to understanding the potential degradation after fire (Kutiel and Inbar 1993, Fox *et al.* 2008) and to comprehending ecosystems' post-fire resilience (Lentile *et al.* 2007).

Fire severity and burn severity assessments are two different approaches to quantify the impact of fire, describing the amount of damage (Hammill and Bradstock 2006), the physical, chemical and biological changes (Chafer *et al.* 2004, Cocke *et al.* 2005) or the

---

\*Corresponding author. Email: Sander.S.Veraverbeke@jpl.nasa.gov

degree of alteration (Brewer *et al.* 2005) that fire causes to an ecosystem. Fire severity quantifies the short-term fire effects in the immediate post-fire environment (Lentile *et al.* 2006) and is usually measured in an initial assessment scheme (Key and Benson 2005). As such, it mainly quantifies vegetation consumption and soil alteration. Burn severity, on the other hand, quantifies both the short- and the long-term impact as it includes response processes (e.g. resprouting, delayed mortality), which is evaluated in an extended assessment (EA) that incorporates both first- and second-order effects (Lentile *et al.* 2006). In this study, burn severity defined as the degree of environmental change caused by a fire (Key and Benson 2005) is estimated one year post-fire.

Several remote sensing studies have discussed the potential of satellite imagery as an alternative for extensive field sampling to quantify both fire and burn severity over large areas. These studies evaluated the use of spectral unmixing (Rogan and Yool 2001, Lewis *et al.* 2007), simulation techniques (Chuvieco *et al.* 2006, De Santis and Chuvieco 2007) and spectral indices to assess fire/burn severity (for a comprehensive review of remote sensing techniques for fire/burn severity assessment, see French *et al.* 2008). These spectral indices were based on normalized difference spectral indices (NDSIs), such as the Normalized Difference Vegetation Index (NDVI) (e.g. Chafer *et al.* 2004, Hammill and Bradstock 2006) or the widely used Normalized Burn Ratio (NBR) (e.g. Lopez-Garcia and Caselles 1991, Epting *et al.* 2005, Key and Benson 2005, Miller and Thode 2007). The NDVI combines the reflectance in the R (red) and NIR (near-infrared) spectral region and is a measure for the amount of green vegetation, whereas the NBR relates to vegetation moisture by combining the NIR with MIR (mid-infrared) reflectance (Gao 1996). Since fire effects on vegetation produce a reflectance increase in the R and MIR spectral regions and an NIR reflectance drop (Pereira *et al.* 1999), bi-temporal image differencing is frequently applied on pre- and post-fire NDVI or NBR images. This results respectively in the differenced Normalized Difference Vegetation Index (dNDVI) (Chafer *et al.* 2004, Hammill and Bradstock 2006) and the differenced Normalized Burn Ratio (dNBR) (Key and Benson 2005). The advantage of these pre/post-fire differenced indices is that they permit a clear discrimination between unburned sparsely vegetated areas and burnt areas, which is difficult in mono-temporal imagery (Key and Benson 2005). Additionally, Miller and Thode (2007) proposed a relative version of the dNBR (RdNBR). This index takes into account the pre-fire amount of biomass, and therefore, rather than being a measure of absolute change, reflects the change caused by fire relative to the pre-fire condition.

Field data are used to evaluate the proposed remotely sensed indices for estimating fire/burn severity, ranging from accuracy assessments on index-based severity classifications (e.g. White *et al.* 1996, Chafer *et al.* 2004, Epting *et al.* 2005, Hammill and Bradstock 2006) to empirical fitting models between spectral indices and field measurements. In this context, a wide range of field data has been considered: % live trees (Lopez-Garcia and Caselles 1991, Alleaume *et al.* 2005) or % tree mortality (Kushla and Ripple 1998), basal area mortality (Chappel and Agee 1996) combustion completeness (Alleaume *et al.* 2005), changes in Leaf Area Index (LAI) (Boer *et al.* 2008) and fractional cover of several components (Lewis *et al.* 2007). However, by far the most widely used field measurement is the Composite Burn Index (CBI) (Key and Benson 2005). The CBI is a semi-quantitative field sampling approach based on an expert judgement procedure, developed as an operational methodology for validating remotely sensed assessments of fire/burn severity on a national scale in the United States as part of the FIREMON (Fire Effects Monitoring and Inventory Protocol) project. Recently, De Santis and Chuvieco (2009) developed GeoCBI (Geo

Composite Burn Index), a modified version of the CBI that accounts for the fraction of coverage (FCOV) of the different vegetation strata. Although the relationship between the CBI and several spectral indices has been recently confirmed by empirical fitting for many vegetation types in the North American boreal region (Epting *et al.* 2005, Allen and Sorbel 2008, Hall *et al.* 2008, Hoy *et al.* 2008, Murphy *et al.* 2008), no uniform relationship could be established. The CBI-dNBR relationship showed large dependencies on pre-fire land cover type (Key and Benson 2005, French *et al.* 2008) and the regression model used (Hall *et al.* 2008). Consequently, it is essential to independently validate the spectral-indices-based burn severity approach with field data for specific regions and vegetation types (Cocke *et al.* 2005, Key and Benson 2005, Lentile *et al.* 2006, Fox *et al.* 2008) to: (i) determine if the technique is capable of producing information relevant to burn severity assessment (French *et al.* 2008) and (ii) quantify the relationship between field data and burn severity measurements derived from satellite imagery. To our knowledge outside North America, only one study (De Santis and Chuvieco 2007) ascertained the empirical relationship between CBI field data and spectral indices. As the technique is conceptually and computationally easy, burn severity maps based on spectral indices could form an important instrument for post-fire management practices in the fire-prone Mediterranean biome. As the patchy and heterogeneous nature of the Mediterranean landscape potentially influences the relationship between field data and spectral indices, there is a need to validate independently the approach in this ecoregion. Therefore, the primary objectives of this study are (i) to evaluate the relationship of several pre/post-fire differenced spectral indices, including the dNBR, the RdNBR and the dNDVI, against GeoCBI field data in the fire-prone biome of the Mediterranean Basin; (ii) to test this relation for specific land cover types and (iii) to examine the influence of the regression model type (linear versus nonlinear).

## 2. Material and methods

### 2.1 Study area

The study area is situated at the Peloponnese peninsula, in southern Greece ( $36^{\circ} 30' - 38^{\circ} 30' \text{ N}$ ,  $21^{\circ} - 23^{\circ} \text{ E}$ ) (see figure 1). The topography is rugged with elevations ranging between 0 and 2404 m above sea level. The climate is typically Mediterranean with hot, dry summers and mild, wet winters. For the Kalamata meteorological station ( $37^{\circ} 4' \text{ N}$ ,  $22^{\circ} 1' \text{ E}$ ) the average annual temperature is  $17.8^{\circ}\text{C}$  and the mean annual precipitation equals 780 mm (Hellenic National Meteorological Service, [www.hnms.gr](http://www.hnms.gr)).

In the 2007 summer, after a severe drought period, large wildfires struck the Peloponnese. The fires consumed a large amount (more than 100 000 ha) of coniferous forest, broadleaved forest, shrub lands (maquis and phrygana communities) and olive groves. Black pine (*Pinus nigra*) is the dominant conifer species. The shrub layer can be divided into maquis and phrygana communities. Maquis communities consist of sclerophyllous evergreen shrubs 2–3 m high (Polunin 1980). Phrygana is dwarf scrub vegetation (<1 m) that prevails on dry landforms (Polunin 1980). The shrub layer is characterized by, for example, Kermes oak (*Quercus coccifera*), Hungarian oak (*Q. frainetto*), mastic tree (*Pistacia lentiscus*), sageleaf rockrose (*Cistus salvifolius*), hairy rockrose (*C. incanus*), tree heath (*Erica arborea*) and thorny burnet (*Sarcopoterium spinosum*). The olive groves consist of *Olea europaea* trees whereas oaks are the dominant broadleaved species.

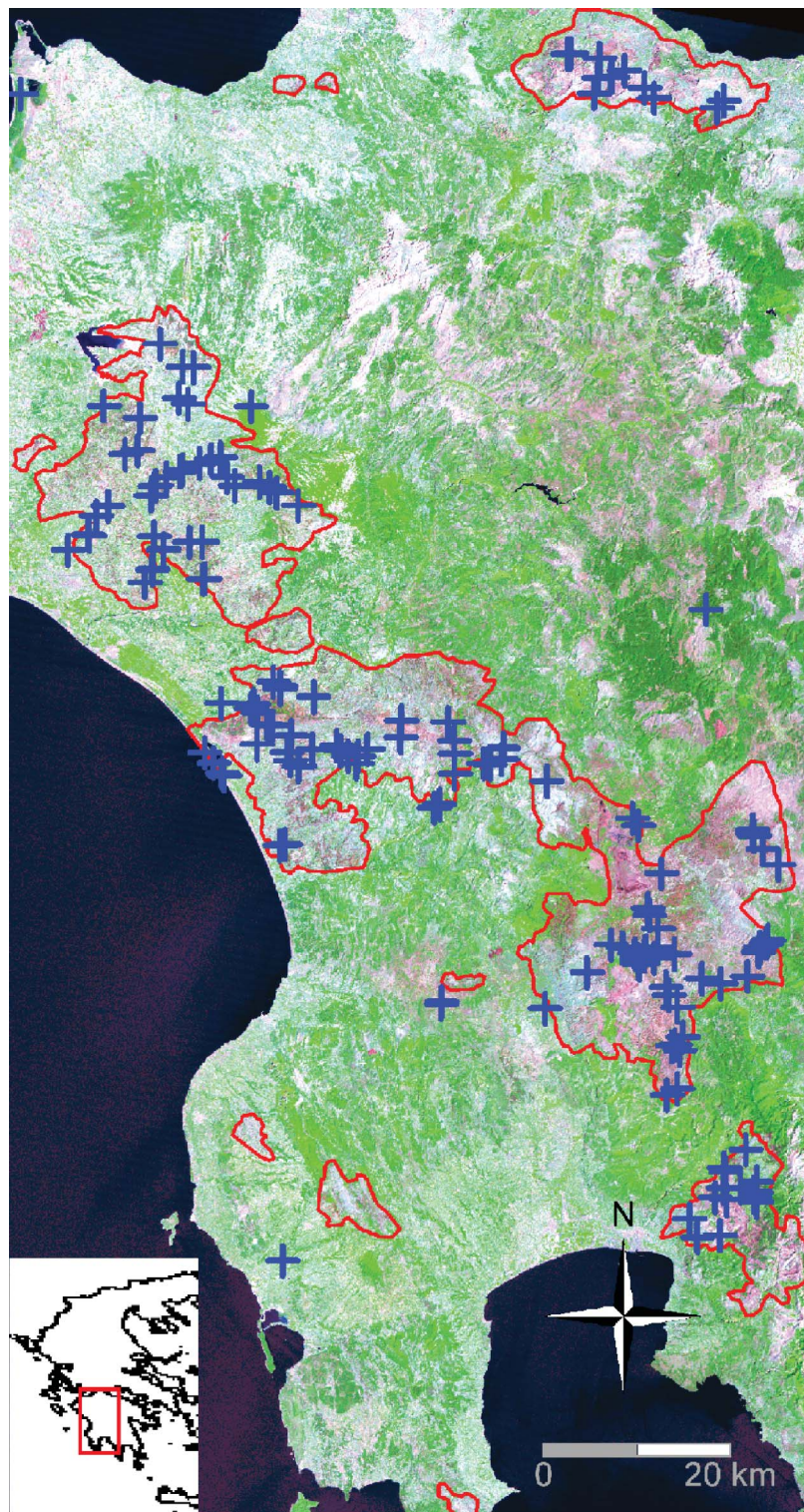


Figure 1. Location of the study area and field plot distribution (Landsat TM 13 August 2008, RGB-743).

## 2.2 Field data

To assess burn severity in the field, field data were collected in September 2008, that is, one year post-fire. The field data consist of 160 GeoCBI (Geo Composite Burn Index) plots. The GeoCBI is a modified version of the Composite Burn Index (CBI) (De Santis and Chuvieco 2009). The (Geo)CBI is an operational tool used in conjunction with the Landsat dNBR approach to assess burn severity in the field (Key and Benson 2005). The GeoCBI divides the ecosystem into five different strata, one for the substrates and four vegetation layers. These strata are: (i) substrates; (ii) herbs, low shrubs and trees less than 1 m; (iii) tall shrubs and trees of 1–5 m; (iv) intermediate trees of 5–20 m and (v) large trees higher than 20 m. In the field form, 20 different factors can be rated (e.g. soil and rock cover/colour change, % LAI change, char height) (see table 1) but only those factors present and reliably rateable are considered. The rates are given on a continuous scale between 0 and 3 and the resulting factor ratings are averaged per stratum. Based on these stratum averages, the GeoCBI is calculated in proportion to their corresponding fraction of cover, resulting in a weighted average between zero and three which expresses burn severity.

The 160 sample points were selected based on a stratified sampling approach, taking into account the constraints mainly on accessibility and time; these points encompass the whole range of variation found within the burns. Contributing to this objective, 10 out of the 160 plots were measured in unburned land, with a consequent GeoCBI value of zero. The field plots consisted of 30 m × 30 m squares, analogous to the Landsat pixel size. The pixel centre coordinates were recorded with a hand-held GPS (Global Positioning System) receiver. The plots were at least 90 m apart and chosen in relatively homogeneous areas of at least 60 m × 60 m, although preferably more (Key and Benson 2005). This homogeneity refers to both the fuel type and the fire effects. Of the 160 field plots 67 plots were measured in shrub land, 58 in coniferous forest, 17 in broadleaved forest and 18 in olive groves. The photographs in figure 2 show examples of low, moderate and high severity plot for the most prevailing fuel types, namely coniferous forest and shrub land.

## 2.3 Imagery and preprocessing

For assessing burn severity of the summer 2007 (July and August) Peloponnese fires two anniversary date Landsat TM images with path/row 184/34 were used (23 July 2006 and 13 August 2008). The images were acquired in summer season, minimizing effects of vegetation phenology and differing solar zenith angles. The images were subjected to geometric, radiometric, atmospheric correction and topographic correction.

The 2008 image was geometrically corrected using 34 ground control points (GCPs), recorded in the field with a GPS receiver. The resulting root mean square error (RMSE) was 0.42 pixels. The 2006 and 2008 images were co-registered with a 0.37 pixels RMSE. All images were registered in Universal Transverse Mercator (zone 34S), with ED 50 (European Datum 1950) as geodetic datum.

To convert the raw digital numbers (DN) to reflectance values the COST method of Chavez (1996) was used:

$$\rho_a = \frac{\pi(L_s - L_d)}{(E_o / -d^2)(\cos \theta_z)^2}, \quad (1)$$

Table 1. GeoCBI criteria used to estimate burn severity in the field (after De Santis and Chuvieco 2009).

Stratum		Burn severity scale					
		No effect			Moderate		
		0	0.5	1	1.5	2	2.5
<b>Substrates</b>							
Litter (l) / light fuel (lf)	Consumed (%)	0	—	50% l	—	100% lf	>80% lf
Duff (%)	0	—	—	Light char	—	—	Consumed >60
Medium/heavy fuel (%)	0	—	—	20	—	—	>80
Soil & rock cover/colour (%)	0	—	—	10	—	—	—
<b>Herbs, low shrubs and trees &lt; 1 m</b>							
Foliation altered (%)	0	—	—	30	—	80	95
Frequency living (%)	100	—	—	90	—	50	95
New sprouts	Abundant	—	—	Moderate-high	—	Moderate	<20
<b>Tall shrubs and trees 1–5 m</b>							
Foliation altered (%)	0	—	—	20	—	60–90	>95
Frequency living (%)	100	—	—	90	—	30	<15
LAI change	0	—	—	15	—	70	90
<b>Intermediate trees 5–20 m</b>							
Green (unaltered) (%)	100	—	—	80	—	40	<10
Black/brown (%)	0	—	—	20	—	60–90	>95
Frequency living (%)	100	—	—	90	—	30	<15
LAI change (%)	0	—	—	15	—	70	90
Char height (m)	None	—	—	1.5	—	2.8	—
<b>Big trees &gt;20 m</b>							
Green (unaltered) (%)	100	—	—	80	—	50	<10
Black/brown (%)	0	—	—	20	—	60–90	>95
Frequency living (%)	100	—	—	90	—	30	<15
LAI change (%)	0	—	—	15	—	70	90
Char height (m)	None	—	—	1.8	—	4	—

Notes: FCOV, fraction of coverage.

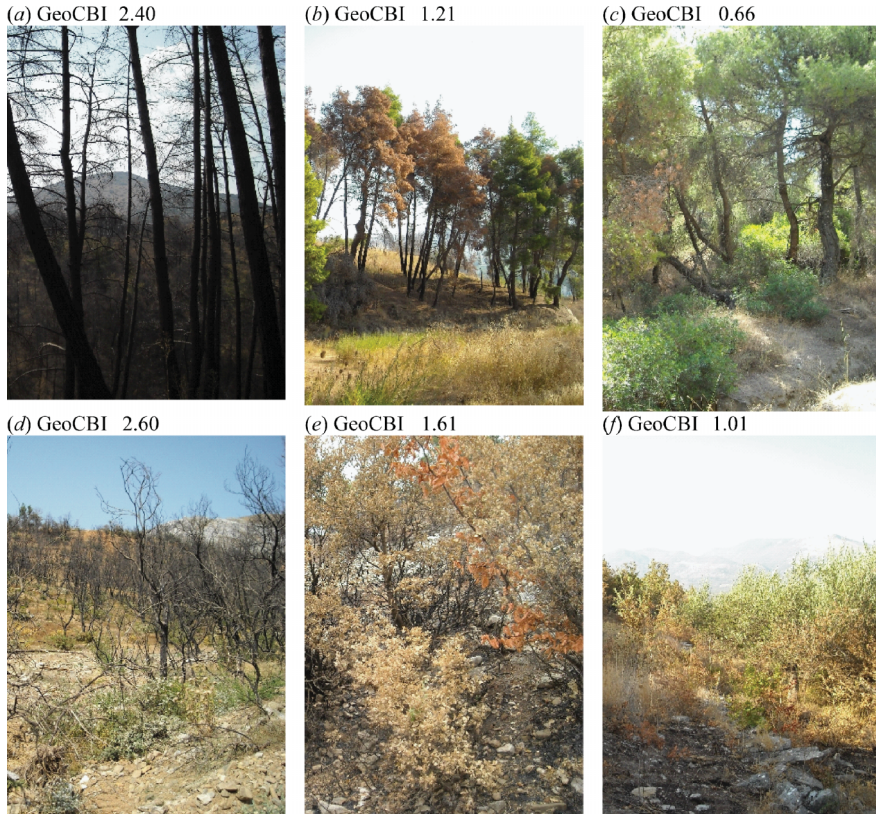


Figure 2. High, moderate and low severity plot in coniferous forest (*a*, *b*, *c*) and a high, moderate and low severity plot in shrub land (*d*, *e* and *f*).

where  $\rho_a$  is the atmospherically corrected reflectance at the surface;  $L_s$  is the at-sensor radiance ( $\text{W m}^{-2} \text{sr}^{-1}$ );  $L_d$  is the path radiance ( $\text{W m}^{-2} \text{sr}^{-1}$ );  $E_o$  is the solar spectral irradiance ( $\text{W m}^{-2}$ );  $d$  is the Earth–Sun distance (astronomical units) and  $\theta_z$  is the solar zenith angle. The COST method is a dark object subtraction (DOS) approach that assumes 1% surface reflectance for dark objects (e.g. deep water). Band-specific parameters to calculate the at-sensor radiance were provided by the European Space Agency (ESA, [http://earth.esa.int/pub/ESA\\_DOC](http://earth.esa.int/pub/ESA_DOC)). After applying the COST atmospheric correction, pseudo-invariant features (PIFs), such as deep water and bare soil pixels, were inspected in the images. No further relative normalization between the images was considered.

It was necessary to correct for different illumination effects due to topography. This was done based on the C correction method (Teillet *et al.* 1982) using a digital elevation model (DEM) and knowledge of the solar zenith and azimuth angle at the moment of image acquisition. Topographical slope and aspect data were derived from 90 m SRTM (Shuttle Radar Topography Mission) elevation data (Jarvis *et al.* 2006) resampled and coregistered with the Landsat images. The illumination is modelled as

$$\cos \gamma_i = \cos \theta_p \cos \theta_z + \sin \theta_p \sin \theta_z \cos(\phi_a - \phi_o), \quad (2)$$

where  $\gamma_i$  is the incident angle (angle between the normal to the ground and the sun rays);  $\theta_p$  is the slope angle;  $\theta_z$  is the solar zenith angle;  $\phi_a$  is the solar azimuth angle and  $\phi_o$  is the aspect angle. Then the terrain-corrected reflectance  $\rho_t$  is defined as:

$$\rho_t = \rho_a \left( \frac{\cos \theta_z + c_k}{\cos \gamma_i + c_k} \right), \quad (3)$$

where  $c_k$  is a band-specific parameter  $c_k = b_k/m_k$ , for  $\rho_a = b_k + m_k \cos \gamma_i$ . Since topographic normalization works better when applied separately for specific land cover types (Bishop and Colby 2002), burnt area specific  $c$ -values were calculated by masking the burnt area after manual digitization.

## 2.4 Spectral indices

In this study the potential of three Normalized Difference Spectral Indices (NDSIs) for assessing burn severity is evaluated using the TM bands that are most sensitive to post-fire reflectance changes: TM3 (630–690 nm), TM4 (760–900 nm), TM5 (1550–1750 nm) and TM7 (2080–2350 nm). Reflectance in the visual (TM3) and mid-infrared (TM5 and TM7) regions increases after fire, while the NIR region (TM4) is characterized by a reflectance drop (Pereira *et al.* 1999). To capture this information, the NDVI combines R (TM3) band with NIR (TM4) band information, whereas the Normalized Difference Moisture Index (NDMI) (Wilson and Sader 2002) and the NBR combine the NIR (TM4) band with an MIR (TM5 and TM7, respectively) band. The NBR has become the standard spectral index for assessing burn severity, especially in North American regions, whereas the NDMI has not been evaluated before for burn severity applications. Nevertheless, Tucker (1980) suggested that TM5 is well suited for remote sensing of canopy water content. Consequently, it might also reflect post-fire reflectance changes and was included in this study. Burned land typically has low NDVI, NDMI and NBR values.

To determine the magnitude of change caused by fire, the post-fire image is subtracted from the pre-fire image. After bi-temporal differencing, burned land is associated with high values in the dNDVI, differenced NDMI (dNDMI) and dNBR maps. The relative version of the dNBR (RdNBR) assesses the magnitude of change relative to the pre-fire vegetation condition by dividing the dNBR by the square root of the absolute value of the pre-fire NBR. As a consequence, in heterogeneous landscapes, the severity of fire in

Table 2. Spectral indices used in this study.

NDSI	Pre/post-fire differenced	Relative version
$NDVI = \frac{(TM4) - (TM3)}{(TM4) + (TM3)}$	$dNDVI = (NDVI)_{pre} - (NDVI)_{post}$	$RdNDVI = \frac{dNDVI}{\left[ \frac{abs((NDVI)_{pre})}{dNDVI} \right]^{1/2}}$
$NDMI = \frac{(TM4) - (TM5)}{(TM4) + (TM5)}$	$dNDMI = (NDMI)_{pre} - (NDMI)_{post}$	$RdNDMI = \frac{dNDMI}{\left[ \frac{abs((NDMI)_{pre})}{(dNBR)} \right]^{1/2}}$
$NBR = \frac{(TM4) - (TM7)}{(TM4) + (TM7)}$	$dNBR = (NBR)_{pre} - (NBR)_{post}$	$RdNBR = \frac{dNBR}{\left[ \frac{abs((NBR)_{pre})}{(dNBR)} \right]^{1/2}}$

Notes: *NDSI*, normalized difference spectral index; *NDVI*, normalized difference vegetation index; *NDMI*, normalized difference moisture index; *NBR*, normalized burn ratio.

sparserly vegetated areas can be compared more adequately with the severity of fire in a more lush land cover type. For this case study in a heterogeneous Mediterranean landscape, the RdNBR and analogous relative versions of the dNDVI and dNDMI (RdNDVI and RdNDMI) were tested. In summary, the pre/post-fire differenced spectral indices evaluated in this study are the dNDVI, the dNDMI, the dNBR, the RdNDVI, the RdNDMI and the RdNBR (see table 2).

## 2.5 Statistical analysis

Linear and second-degree polynomial regressions were performed to correlate the spectral indices (independent variables) and GeoCBI field data of fire/burn severity (dependent variables). The relationship between the field data and the remotely sensed indices was evaluated both separately for each fuel type (coniferous forest, broadleaved forest, shrub land and olive groves) and for the pooled dataset.

Regression model results were compared using two goodness-of-fit measures: the coefficient of determination,  $R^2$ , and the RMSE. The coefficient of determination is an estimate of the proportion of the total variation in the data that is explained by the model. The RMSE is a measure of how much a response variable varies from the model predictions, expressed in the same units as the dependent data. The  $R^2$  and the RMSE are to some degree interlinked. A model yielding a high  $R^2$  will generally have a low RMSE and vice versa. However, because the RMSE describes how far points diverge from the regression line, the regression models with equal  $R^2$  values potentially can have quite different RMSEs.

The statistical analysis focused on (i) the differences between the dNDVI, dNDMI and dNBR approaches; (ii) the comparison of the absolute and relative indices; (iii) the fuel-type specific regression models and (iv) the influence of the regression model type.

## 3. Results

### 3.1 Differences between the dNBR, dNDMI and dNDVI approaches

The distribution plots and regression lines of the GeoCBI and absolute pre/post-fire differenced spectral indices are displayed in figure 3(a–c). Comparison of these models shows that the GeoCBI–dNBR relationship proved to be the strongest. This relationship yielded a moderate–high  $R^2 = 0.65$  for a polynomial fitting model. This was followed by the GeoCBI–dNDMI correlation with an  $R^2 = 0.50$ . The GeoCBI–dNDVI relationship was the weakest ( $R^2 = 0.46$ ). The decreasing trend in the  $R^2$  statistic is at the same time associated with an increasing RMSE.

The spectral index values of the dNBR approach clearly range more than those of the dNDMI and dNDVI approaches. The within-burn dNBR range almost doubles the within-burn dNDVI range. Most field plots have dNBR values ranging from 0 and 0.8 (see figure 3(c)) and dNDMI and dNDVI between 0 and 0.5 (see figure 3(a), and (b)). Figure 4(a–c) depict the dNDVI, dNDMI and dNBR maps, respectively. The dNBR map clearly reveals more contrast in the burnt areas than the other maps.

### 3.2 Absolute versus relative indices

Two main differences can be seen when comparing absolute and relative differenced indices. Firstly, the range of the RdNDMI and the RdNBR (see figure 3(e) and (f)) is markedly larger in comparison with their absolute counterparts (see figure 3(b) and (c)) with index values ranging between 0 and 1. This is not the case for the RdNDVI (see figure

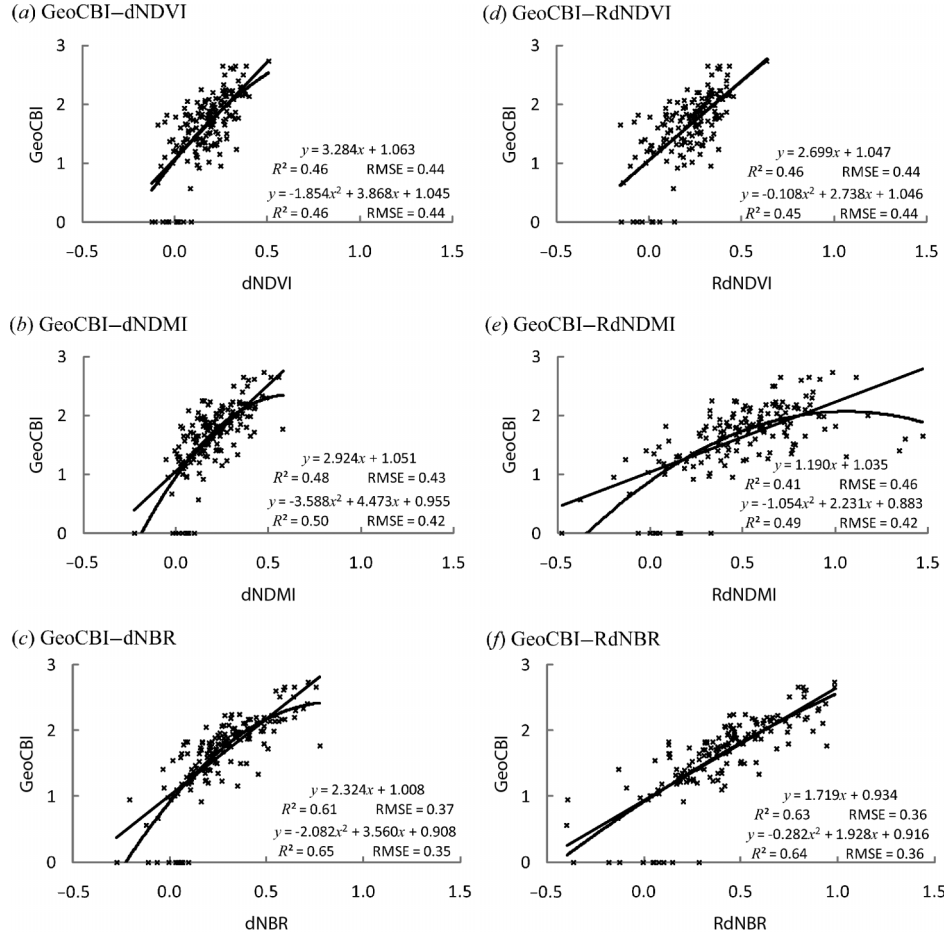


Figure 3. Distribution plots and regression lines for (a) GeoCBI-dNDVI, (b) GeoCBI-dNDMI, (c) GeoCBI-dNBR, (d) GeoCBI-RdNDVI, (e) GeoCBI-RdNDMI and (f) GeoCBI-RdNBR.

3(d)) index values, which range from 0 to 0.5, similar to the dNDVI (see figure 3(a)). Secondly, the empirical models for the relative approaches provided slightly poorer results than their absolute equivalents with a GeoCBI-RdNBR  $R^2 = 0.64$ , a GeoCBI-RdNDMI  $R^2 = 0.49$  and a GeoCBI-RdNDVI  $R^2 = 0.45$ . Figure 4(d–f) display, respectively, the RdNDVI, RdNDMI and RdNBR maps. Within-burn contrast is the highest in the RdNBR map, followed by the RdNDMI and RdNDVI maps.

### 3.3 Fuel type specific regression models

Burn severity was estimated most accurately for the olive groves class ( $R^2 = 0.95$ ), followed by coniferous forest ( $R^2 = 0.72$ ), broadleaved forest ( $R^2 = 0.66$ ) and shrub land ( $R^2 = 0.56$ ) (GeoCBI-dNBR correlations; see table 3). The remarkably high correlation between the field data and the dNBR for olive groves is a striking result. However, care must be taken when interpreting the results of the broadleaved forest and olive groves fuel types, as only a limited number of field plots were sampled in these land cover types ( $n = 17$  and  $n = 18$ , respectively).

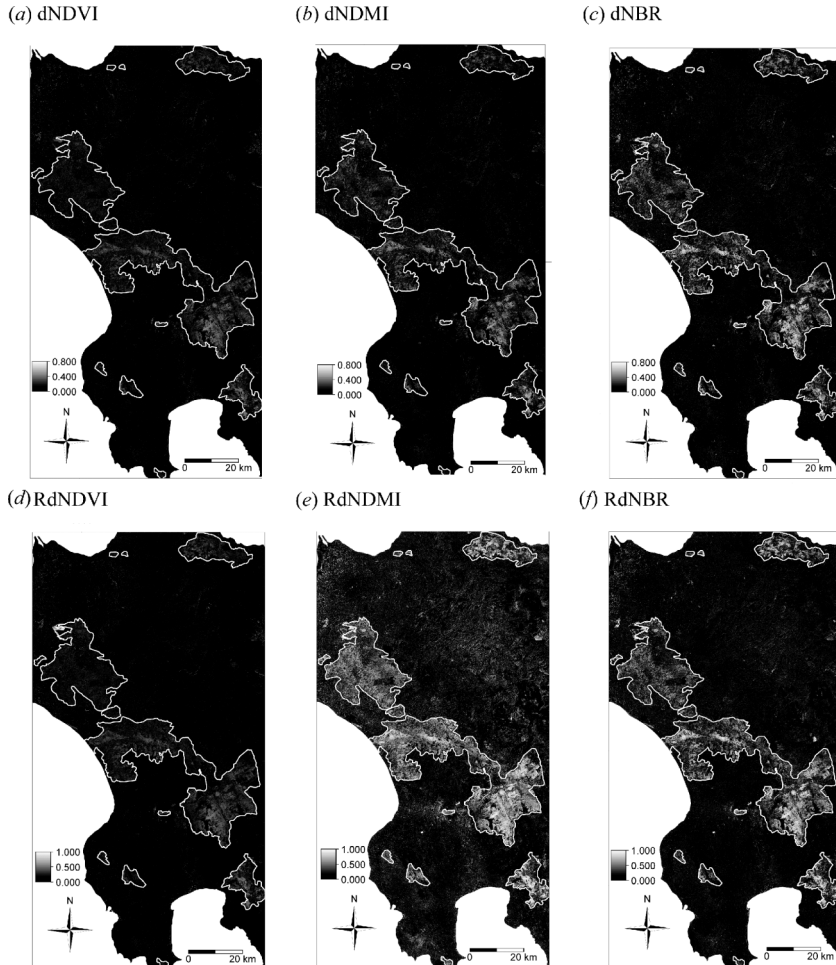


Figure 4. Severity maps for (a) dNDVI, (b) dNDMI, (c) dNBR, (d) RdNDVI, (e) RdNDMI and (f) RdNBR.

### 3.4 Linear versus polynomial regression models

Second-order polynomial regression models consistently yielded better results than linear models for the NBR and NDMI approaches. For the NDVI approaches, the polynomial model did not improve the linear model.

## 4. Discussion

### 4.1 Differences between the dNBR, dNDMI and dNDVI approaches

The dNBR approach gave the overall best correlation with GeoCBI field data, followed by the dNDMI and the dNDVI approach. Indices with a mid-infrared spectral band yielded better results than indices lacking an MIR band. This corroborates earlier research findings. Pereira (1999) reported that AVHRR (Advanced Very High Resolution Radiometer) spectral indices based on the NIR and MIR channels

Table 3. Land cover-specific modelling results with regression model significance level of  $p < 0.01$ .

Model form	Shrub land ( $n = 67$ )				Coniferous forest ( $n = 58$ )				Broadleaved forest ( $n = 17$ )				Olive groves ( $n = 18$ )	
	RMSE	$R^2$	RMSE	$R^2$	RMSE	$R^2$	RMSE	$R^2$	RMSE	$R^2$	RMSE	$R^2$	RMSE	$R^2$
GeoCBI-dNBR linear	0.36	0.55	0.34	0.69	0.47	0.61	0.24	0.81						
GeoCBI-dNBR polynomial	0.36	0.56	0.32	0.72	0.47	0.66	0.13	0.95						
GeoCBI-dNDMI linear	0.39	0.46	0.38	0.60	0.53	0.51	0.43	0.39						
GeoCBI-dNDMI polynomial	0.39	0.48	0.37	0.62	0.55	0.51	0.39	0.53						
GeoCBI-dNDVI linear	0.41	0.41	0.39	0.58	0.54	0.49	0.45	0.34						
GeoCBI-dNDVI polynomial	0.41	0.43	0.38	0.60	0.54	0.53	0.41	0.50						
GeoCBI-RdNBR linear	0.37	0.51	0.33	0.70	0.44	0.66	0.22	0.85						
GeoCBI-RdNBR polynomial	0.37	0.52	0.32	0.72	0.45	0.67	0.13	0.95						
GeoCBI-RdNDMI linear	0.47	0.22	0.39	0.59	0.56	0.45	0.41	0.45						
GeoCBI-RdNDMI polynomial	0.42	0.39	0.38	0.62	0.57	0.47	0.35	0.62						
GeoCBI-RdNDVI linear	0.42	0.39	0.39	0.58	0.52	0.53	0.45	0.36						
GeoCBI-RdNDVI polynomial	0.41	0.42	0.39	0.60	0.53	0.41	0.41	0.50						

had a higher discriminatory potential for burned surface mapping than indices based on the NIR and red channels. Trigg and Flasse (2001) demonstrated the importance of the MIR region for burned shrub–savannah discrimination with MODIS (Moderate Resolution Imaging Spectroradiometer) data. The study of Escuin *et al.* (2008) showed, using Landsat TM/ETM+ images, that the NBR was better suited than the NDVI for discriminating burns and distinguishing different degrees of severity. The results are also consistent with van Wagendonk *et al.* (2004), who found significant post-fire spectral changes using hyperspectral AVIRIS (Airborne Visible and Infrared Imaging Spectroradiometer) data. In previous studies assessing the correlation between several spectral indices and CBI field data, Epting *et al.* (2005) ranked the NBR as the first index in pre/post-burn approaches. Similar findings were obtained by Hoy *et al.* (2008), reporting that dNBR outperforms dNDVI. For fires in several regions in the United States dNBR yielded higher correlations than dNDVI (Zhu *et al.* 2006). In this report the within-burn range of dNDVI values was about half the within-burn range of dNBR values, which is similar to our results. They also concluded that dNDVI was more influenced by hazy conditions due to the elevated potential of atmospheric scattering in the red spectral region.

Also NDMI-based approaches, which have not been evaluated before for estimating burn severity, have proven to perform better than NDVI-based approaches. However, the NBR outperformed the NDMI. This can be explained by the typically lower reflectances in Landsat TM band 7 (2080–2350 nm) than in Landsat TM band 5 (1550–1750 nm) due to a higher degree of water absorption by vegetation for longer wavelengths. Therefore, fire-induced reflectance increase is likely to be more explicit in TM7 than in TM5. As a result, an index with TM7 instead of TM5 is able to capture a large range of variation in post-fire effects.

Overall results show a moderate-high correlation between GeoCBI field data and dNBR for this case study in a Mediterranean environment. Polynomial fitting models resulted in  $R^2 = 0.65$ . These outcomes fall within the range of results of previous studies (French *et al.* 2008).

#### 4.2 Absolute versus relative indices

The relative indices resulted in similar or even slightly poorer correlations between the remotely sensed indices and the GeoCBI field data in comparison with their absolute equivalents. This is a marked outcome as RdNBR was developed as a major improvement on the dNBR approach for heterogeneous landscapes (Miller and Thode 2007). The RdNBR improved the burn severity mapping in the MTE of California, USA. The landscape of the Peloponnese is a typical Mediterranean environment with its heterogeneous and patchy characteristics. The Peloponnese 2007 fires consumed a mixture of forest, shrub land and agricultural land. Even within each fuel type, we observed a large range of variation. For example, shrub density and shrub height in shrub land differ largely in the study area. This is a classic example environment where the relative index is expected to improve the burn severity assessment. But overall, and even for the shrub-land-specific regressions, absolute indices outperformed their relative equivalents. Dividing the difference maps by the square root of the absolute value of the pre-fire index value enlarges the within-burn index range (see figure 3(e) and (f)). Apparently, however, that does not influence the assessment in a beneficial way in our case study. Thus, despite their theoretical strength, relative indices did not perform better than their absolute counterparts in our study. Zhu *et al.*

(2006) also concluded that for different ecosystems across the United States, including California, RdNBR trended slightly poorer with CBI field data than dNBR. Another problem associated with the relative index is that dividing by a close-to-zero value results in unrealistic high positive or low negative relative index values that lose their linkage with burn severity. When pre-fire index values are low over significantly extensive areas, this can result in speckled images. We recommend an in-depth evaluation of the relative indices, especially the RdNBR, in more case studies to determine if the theoretical improvement of the RdNBR translates into a consistent improvement in heterogeneous landscapes.

#### **4.3 Fuel-type-specific regression models**

The strength of the GeoCBI–dNBR relationship is also influenced by pre-fire vegetation type. Hall *et al.* (2008) advise a stratified sampling scheme, not only covering the whole range of severity, but also equally representing the fuel types prevailing in the study area. This could be a major improvement for burn severity modelling. However, in practice it is sometimes not possible to sample each land cover class equally. Nevertheless, in our study the number of samples of each fuel type is more or less proportional to the total area burned of the different fuel types. Results of the less sampled broadleaved forest and olive groves classes must be handled with care.

Model results vary by fuel type. Epting *et al.* (2005) found a rather strong correlation between field data and spectral indices for forested classes. More sparsely vegetated classes (e.g. shrubs, herbs) underperformed. Allen and Sorbel (2008) found deciduous and tundra plots not having an equally strong correlation between dNBR and CBI as observed in black spruce plots. Zhu *et al.* (2006) also found the correlations in forest land clearly stronger than those in sparser vegetation types. In our study the general experience from previous studies that forested classes have higher performances in estimating burn severity than more sparsely vegetated areas is confirmed. The fuel types are ranked based on their GeoCBI–dNBR correlation as shrub land, coniferous forest, broadleaved forest and olive groves (see table 3). The GeoCBI–dNBR correlation was unexpectedly high for the olive grove samples with an  $R^2$  even higher than for natural vegetation types. This potentially reveals the strengths of the multi-strata CBI approach to assess burn severity in any vegetation type, even in cultural landscapes. This is certainly an important advantage for assessing post-fire effects in environments, such as the Mediterranean region, where man created many patches of cultural landscape in a matrix of natural vegetation.

#### **4.4 Linear versus polynomial regression models**

The regression model type, linear versus nonlinear, is another factor that affects the degree of correlation. Previous research (van Wagendonk *et al.* 2004) showed that the relationship between dNBR and CBI field data is clearly nonlinear. Polynomial models result in higher coefficients of determination and lower RMSEs than linear regression models (van Wagendonk *et al.* 2004, Hall *et al.* 2008). The CBI–dNBR relationship, however, tends to saturate for CBI values that are higher than 2.5 (van Wagendonk *et al.* 2004). Therefore Hall *et al.* (2008) proposed a saturated growth model that lacks this unwanted feature. However,  $R^2$  values obtained by the saturated growth model are slightly lower than those of second-order polynomial models. In our study, we evaluated both linear and second-order polynomial models. Polynomial models gave significantly better results for NBR- and NDMI-based approaches (see

figure 3(b) and (c)). For these indices, the relationship with the field data is clearly nonlinear. The polynomial model indeed saturates for GeoCBI values higher than 2.3. For the NDVI approach, the linear model performed as well as the polynomial model. The relationship between the NDVI-based measures and the field data appears to be linear, in contrast to the NBR and NDMI.

## 5. Conclusions

Indices based on an MIR–NIR band combination, the NBR and NDMI, gave better results than the NDVI for assessing burn severity. The GeoCBI–dNBR relationship proved to be the strongest, yielding a moderate–high  $R^2 = 0.65$  for this case study in the Peloponnese, a Mediterranean type ecosystem. Although theoretically adapted to the characteristics of the study area, relative indices that account for pre-fire vegetation state did not perform better than their absolute equivalents. The relationship between the remotely sensed indices was stronger for forest ecotypes than for more sparsely vegetated areas, except for the high correlation ( $R^2 = 0.95$ ) in olive groves. These results reveal the potential of the multi-layered CBI approach allowing any land cover type, whether or not natural. The relationship between the field data and the NBR and NDMI indices derived from remote sensing was clearly nonlinear, in contrast to the GeoCBI–dNDVI linear relationship.

## Acknowledgement

The study was financed by the Ghent University special research funds (BOF: Bijzonder Onderzoeksfonds).

## References

- ALLEAUME, S., HELY, C., LE ROUX, C., KORONTZI, S., SWAP, R., SHUGART, H. and JUSTICE, C., 2005, Using MODIS to evaluate heterogeneity of biomass burning in southern African savannahs: a case study. *International Journal of Remote Sensing*, **26**, pp. 4219–4237.
- ALLEN, J. and SORBEL, B., 2008, Assessing the differenced Normalized Burn Ratio's ability to map burn severity in the boreal forest and tundra ecosystems of Alaska's national parks. *International Journal of Wildland Fire*, **17**, pp. 463–475.
- BISHOP, M. and COLBY, J., 2002, Anisotropic reflectance correction of SPOT-3 HRV imagery. *International Journal of Remote Sensing*, **23**, pp. 2125–2131.
- BOER, M., MACFARLANE, C., NORRIS, J., SADLER, R., WALLACE, J. and GRIERSON, P., 2008, Mapping burned areas and burn severity patterns in SW Australian eucalypt forest using remotely-sensed changes in leaf area index. *Remote Sensing of Environment*, **112**, pp. 4358–4369.
- BREWER, K., WINNE, C., REDMOND, R., OPITZ, D. and MANGRICH, M., 2005, Classifying and mapping wildfire severity: a comparison of methods. *Photogrammetric Engineering & Remote Sensing*, **71**, pp. 1311–1320.
- CAPITANIO, R. and CARCAILLET, C., 2008, Post-fire Mediterranean vegetation dynamics and diversity: a discussion of succession models. *Forest Ecology and Management*, **255**, pp. 431–439.
- CHAFER, C., NOONAN, M. and MAGNAUGHT, E., 2004, The post-fire measurement of fire severity and intensity in the Christmas 2001 Sydney wildfires. *International Journal of Wildland Fire*, **13**, pp. 227–240.
- CHAPPEL, C. and AGEE, J., 1996, Fire severity and tree seedling establishment in *Abies Magnifica* Forests, Southern Cascades, Oregon. *Ecological Applications*, **6**, pp. 628–640.
- CHAVEZ, P., 1996, Image-based atmospheric corrections – revisited and improved. *Photogrammetric Engineering & Remote Sensing*, **62**, pp. 1025–1036.

- CHUVIECO, E., RIANO, D., DANSON, F. and MARTIN, P., 2006, Use of a radiative transfer model to simulate the postfire spectral response to burn severity. *Journal of Geophysical Research*, **111**, G04S09.
- COCKE, A., FULE, P. and CROUSE, J., 2005, Comparison of burn severity assessments using Differenced Normalized Burn Ratio and ground data. *International Journal of Wildland Fire*, **14**, pp. 189–198.
- DE SANTIS, A. and CHUVIECO, E., 2007, Burn severity estimation from remotely sensed data: performance of simulation versus empirical models. *Remote Sensing of Environment*, **108**, pp. 422–435.
- DE SANTIS, A. and CHUVIECO, E., 2009, GeoCBI: a modified version of the Composite Burn Index for the initial assessment of the short-term burn severity from remotely sensed data. *Remote Sensing of Environment*, **113**, pp. 554–562.
- EPTING, J., VERBYLA, D. and SORBEL, B., 2005, Evaluation of remotely sensed indices for assessing burn severity in interior Alaska using Landsat TM and ETM+. *Remote Sensing of Environment*, **96**, pp. 328–339.
- ESCUIN, S., NAVARRO, R. and FERNANDEZ, P., 2008, Fire severity assessment by using NBR (Normalized Burn Ratio) and NDVI (Normalized Difference Vegetation Index) derived from LANDSAT TM/ETM images. *International Journal of Remote Sensing*, **29**, pp. 1053–1073.
- FOX, D., MASELLI, F. and CARREGA, P., 2008, Using SPOT images and field sampling to map burn severity and vegetation factors affecting post forest fire erosion risk. *Catena*, **75**, pp. 326–335.
- FRENCH, N., KASISCHKE, E., HALL, R., MURPHY, K., VERBYLA, D., HOY, E. and ALLEN, J., 2008, Using Landsat data to assess fire and burn severity in the North American boreal forest region: an overview and summary of results. *International Journal of Wildland Fire*, **17**, pp. 443–462.
- GAO B., 1996, NDWI-A Normalized Difference Water Index for remote sensing of vegetation liquid water from space. *Remote Sensing of Environment*, **58**, pp. 257–266.
- HALL, R., FREEBURN, J., DE GROOT, W., PRITCHARD, J., LYNHAM, T. and LANDRY, R., 2008, Remote sensing of burn severity: experience from western Canada boreal fires. *International Journal of Wildland Fire*, **17**, pp. 476–489.
- HAMMILL, K. and BRADSTOCK, R., 2006, Remote sensing of fire severity in the Blue Mountains: influence of vegetation type and inferring fire intensity. *International Journal of Wildland Fire*, **15**, pp. 213–226.
- HOY, E., FRENCH, N., TURETSKY, M., TRIGG, S. and KASISCHKE, E., 2008, Evaluating the potential of Landsat TM/ETM+ imagery for assessing fire severity in Alaskan black spruce forest. *International Journal of Wildland Fire*, **17**, pp. 500–514.
- JARVIS, A., REUTER, H., NELSON, A. and GEUVARA, E., 2006, Hole-filled seamless SRTM data V3. International Centre for Tropical Agriculture (CIAT). Available online at: <http://srtm.csi.cgiar.org> (accessed 11 June 2009).
- KEY, C. and BENSON, N., 2005, Landscape assessment: ground measure of severity; the Composite Burn Index, and remote sensing of severity, the Normalized Burn Index. In *FIREMON: Fire Effects Monitoring and Inventory System*, D. Lutes, R. Keane, J. Caratti, C. Key, N. Benson, S. Sutherland and L. Gangi (Eds.), pp. 1–51 (Ogden, UT: USDA Forest Service, Rocky Mountains Research Station, General Technical Report RMRS-GTR-164-CD LA).
- KUSHLA, J. and RIPPLE, W., 1998, Assessing wildfire effects with Landsat thematic mapper data. *International Journal of Remote Sensing*, **19**, pp. 2493–2507.
- KUTIEL, P. and INBAR, M., 1993, Fire impacts on soil nutrients and soil erosion in a Mediterranean pine forest plantation. *Catena*, **20**, pp. 129–139.
- LENTILE, L., HOLDEN, Z., SMITH, A., FALKOWSKI, M., HUDAK, A., MORGAN, P., LEWIS, S., GESSLER, P. and BENSON, N., 2006, Remote sensing techniques to assess active fire

- characteristics and post-fire effects. *International Journal of Wildland Fire*, **15**, pp. 319–345.
- LENTILE, L., MORGAN, P., HUDAQ, A., BOBBITT, M., LEWIS, S., SMITH, A. and ROBICHAUD, P., 2007, Post-fire burn severity and vegetation response following eight large wildfires across the western United States. *Fire Ecology*, **3**, pp. 91–108.
- LEWIS, S., LENTILE, L., HUDAQ, A., ROBICHAUD, P., MORGAN, P. and BOBBITT, M., 2007, Mapping ground cover using hyperspectral remote sensing after the 2003 Simi and Old wildfires in Southern California. *Journal of Fire Ecology*, **3**, pp. 109–128.
- LOPEZ-GARCIA, M. and CASELLES, V., 1991, Mapping burns and natural reforestation using Thematic Mapper data. *Geocarto International*, **6**, pp. 31–37.
- MILLER, J. and THODE, A., 2007, Quantifying burn severity in a heterogenous landscape with a relative version of the delta Normalized Burn Ratio (dNBR). *Remote Sensing of Environment*, **109**, pp. 66–80.
- MURPHY, K., REYNOLDS, J. and KOLTUN, J., 2008, Evaluating the ability of the differenced Normalized Burn Ratio (dNBR) to predict ecologically significant burn severity in Alaskan boreal forests. *International Journal of Wildland Fire*, **17**, pp. 490–499.
- PAUSAS, J., 2004, Changes in fire and climate in the eastern Iberian peninsula (Mediterranean Basin). *Climatic Change*, **63**, pp. 337–350.
- PEREIRA, J., 1999, A comparative evaluation of NOAA-AVHRR Vegetation Indexes for burned surface detection and mapping. *IEEE Transactions on Geoscience and Remote Sensing*, **37**, pp. 217–226.
- PEREIRA, J., SÁ, A., SOUSA, A., SILVA, J., SANTOS, T. and CARREIRAS, J., 1999, Spectral characterization and discrimination of burnt areas. In *Remote Sensing of Large Wildfires in the European Mediterranean Basin*, E. Chuvieco (Ed.), pp. 123–138 (Berlin: Springer-Verlag).
- POLUNIN, O., 1980, *Flowers of Greece and the Balkans. A field guide*, pp. 1–592 (Oxford: Oxford University Press).
- ROGAN, J. and YOOL, S., 2001, Mapping fire-induced vegetation depletion in the Peloncillo mountains, Arizona and New Mexico. *International Journal of Remote Sensing*, **16**, pp. 3101–3121.
- TEILLET, P., GUINDON, B. and GOODENOUGH, D., 1982, On the slope-aspect correction of multi-spectral scanner data. *Canadian Journal of Remote Sensing*, **8**, pp. 84–106.
- THOMAS, J., WALSH, R. and SHAKESBY, R., 1999, Nutrient losses in eroded sediment after fire in eucalyptus and pine forests in the wet Mediterranean environment of northern Portugal. *Catena*, **36**, pp. 283–302.
- TRABAUD, L., 1981, Man and fire: impacts on Mediterranean vegetation. In *Mediterranean-Type Shrublands*, F. di Castri, D. Goodall and R. Specht (Eds.), pp. 523–537 (Amsterdam: Elsevier)
- TRIGG, S. and FLASSE, S., 2001, An evaluation of different bi-spectral spaces for discriminating burned shrub-savannah. *International Journal of Remote Sensing*, **19**, pp. 3499–3514.
- TUCKER, C., 1980, Remote sensing of leaf water content in the near-infrared. *Remote Sensing of Environment*, **15**, pp. 25–30.
- VAN WAGTENDONK, J., ROOT, R. and KEY, C., 2004, Comparison of AVIRIS and Landsat ETM+ detection capabilities for burn severity. *Remote Sensing of Environment*, **92**, pp. 397–408.
- WHITE, J., RYAN, K., KEY, C. and RUNNING, S. 1996, Remote sensing of forest fire severity and vegetation recovery. *International Journal of Wildland Fire*, **6**, pp. 125–136.
- WILSON, E. and SADER, S., 2002, Detection of forest harvest type using multiple dates of Landsat TM imagery. *Remote Sensing of Environment*, **80**, pp. 385–396.
- ZHU, Z., KEY, C., OHLEN, D. and BENSON, N., 2006, Evaluate sensitivities of burn-severity mapping algorithms for different ecosystems and fire histories in the United States. Final Report to the Joint Fire Science Program: Project JFSP 01-1-4-12(Sioux Falls, SD: US Department of Interior), pp. 1–36.